

Emulsion Polymerization Kinetics and Reactor Design. IV. Continuous-Flow Operation with Recycling

CHEN-CHONG LIN, WEN-YEN CHIU, and LI-CHAU HUANG,
*Department of Chemical Engineering, National Taiwan University, Taipei,
Taiwan, China*

Synopsis

A new mathematical model with a correction for radical capturing efficiency in a continuous emulsion polymerization with recycle flow has been proposed. These performance equations predict the conversion as well as molecular weight distribution of the polymer product during the continuous-flow operation. Experimental results obtained with vigorous mixing associated with a premixer are in best agreement with the theoretical prediction. In certain situations, the recycling provides a means for obtaining a higher degree of back-mixing with a normal flow reactor. However, it is difficult to obtain a high conversion of monomer by a continuous emulsion polymerization operation even with a long residence time. Theoretical and experimental average degrees of polymerization of polymer leaving the reactor are progressively displaced toward smaller values with greater mean residence time. According to the calculations based on our kinetic model, the ratio \bar{M}_w/\bar{M}_n in the continuous emulsion polymerization remains constant regardless of mean residence time.

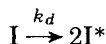
INTRODUCTION

In contrast to batch operation, the kinetics of continuous emulsion polymerization has received scant attention in the literature. Recently, Nomura et al.^{1,2} have proposed a new reaction model based on generating polymer particles for continuous-flow operation in order to analyze the mechanism of continuous emulsion polymerization. It is difficult, however, to predict the molecular weight as well as molecular weight distribution (MWD) during a continuous emulsion polymerization, because of the lack of a suitable and simple mathematical model to describe such a system. We have previously succeeded in establishing³ a mathematical model for continuous emulsion polymerization which can be used to calculate the molecular weight distribution of such reactor systems. In this paper, the effect of the recycling stream on the conversion and the molecular weight distribution is theoretically and experimentally considered in order to validate the proposed reaction model.

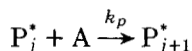
THEORETICAL TREATMENT

Our kinetic scheme of a typical emulsion polymerization can be expressed as follows:

Initiation



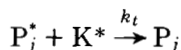
Propagation



Chain Transfer



Termination



where I, K*, A, and P represent the initiator in the reaction system, the initiator radical in the polymer particles, the monomer in the polymer particles, and the polymer itself, respectively. The assumptions made are that (1) the propagation proceeds in the polymer particles, (2) the termination occurs by the collision of polymer radical with initiator radical and chain transfer to monomer, and (3) each polymer particle contains not more than one polymerizing radical. The kinetic equations based on the kinetic scheme have already been developed in our previous paper.³ The essentials are summarized below.

Polymerization Kinetics

A continuous emulsion polymerization of styrene proceeds by complete mixing in a stirred tank with partial recycling. If we neglect the time lag of the recycle stream, the recycling stream has no effect on the kinetic equations. Then the following equations can be obtained:

$$\frac{d[I]}{dt} = \frac{[I_0]}{\bar{\theta}} - \frac{[I]}{\bar{\theta}} - k_d[I] \quad (1)$$

$$\frac{d[I^*]}{dt} = \frac{[I^*]}{\bar{\theta}} + 2k_d\epsilon[I] - k_t[K^*]\hat{P}^* - k_i[K^*][\hat{N} - \hat{P}^*] - \rho_m \quad (2)$$

$$\frac{d[M]}{dt} = \frac{[M_0]}{\bar{\theta}} - \frac{[M]}{\bar{\theta}} - k_p[A]\hat{P}^* - k_{fM}[A]\hat{P}^* \quad (3)$$

$$\begin{aligned} \frac{d[P_1^*]}{dt} = & -\frac{[P_1^*]}{\bar{\theta}} + k_i[K^*][\hat{N} - \hat{P}^*] + \rho_m \\ & - k_p[A][P_1^*] - k_t[K^*][P_1^*] + k_{fM}[A]\hat{P}^* - k_{fM}[A][P_1^*] \quad (4) \end{aligned}$$

$$\frac{d[P_j^*]}{dt} = \frac{[P_j^*]}{\bar{\theta}} + k_p[A][P_{j-1}^*] - k_p[A][P_j^*] - k_i[K^*][P_j^*] - k_{fM}[A][P_j^*] \quad (5)$$

$$\frac{d[P_j]}{dt} = \frac{[P_j]}{\bar{\theta}} + k_t[P_j^*][K^*] + k_{fM}[P_j^*][A] \quad (6)$$

where $\bar{\theta} = V/f$, ϵ = efficiency of initiator, and ρ_m = rate of diffusion of radicals into micelles.

Under steady-state condition, the following equation can be derived from eq. (1):

$$[I] = \frac{[I_0]}{1 + \bar{\theta}k_d} \quad (7)$$

From eqs. (4) and (5),

$$0 = -\frac{\hat{P}^*}{\bar{\theta}} + k_i[K^*][\hat{N} - \hat{P}^*] - k_t[K^*]\hat{P}^* + \rho_m \quad (8)$$

or

$$0 = -\frac{\hat{P}^*}{\bar{\theta}} + (r_i - \rho_m) \frac{\hat{N} - \hat{P}^*}{\hat{N}} - (r_i - \rho_m) \frac{\hat{P}^*}{\hat{N}} + \rho_m \quad (9)$$

where $r_i = 2k_d \epsilon[\text{I}]$. From eq. (9), we obtain

$$\hat{P}^* = 1 / \left(-\frac{1}{r_i \bar{\theta}} + \frac{2}{\hat{N}} \right) \quad (10)$$

Because the value of r_i is on the order of 10^{-5} , \hat{N} is on the order of 10^{-7} , and $\bar{\theta} > 0.5$ (hr) for our experimental conditions, the $1/r_i \bar{\theta}$ term can be neglected in eq. (10). Thus, eq. (10) becomes

$$\hat{P}^* = 0.5 \hat{N} \quad (11)$$

From eqs. (2) and (8), we obtain

$$0 = \frac{[\text{I}^*] + \hat{P}^*}{-\bar{\theta}} + 2k_d \epsilon[\text{I}] - 2k_t [\text{K}^*] \hat{P}^* \quad (12)$$

Because the value of $[\text{I}^*] + \hat{P}^*$ is on the order of $10^{-8} \sim 10^{-7}$ mol/l., $2k_d \epsilon[\text{I}] \sim 2k_t [\text{K}^*] \hat{P}^*$ is on the order of 10^{-5} , and $\bar{\theta} > 0.5$ (hr), the first term of eq. (12) can be neglected. Thus,

$$k_d \epsilon[\text{I}] \cong k_t [\text{K}^*] \hat{P}^* \quad (13)$$

Number of Polymer Particles

$$\frac{d\hat{N}}{dt} = \rho_m \frac{\hat{N}}{\bar{\theta}} \quad (14)$$

Under the steady-state conditions,

$$\hat{N} = \rho_m \bar{\theta} = r_i \bar{\theta} \left(\frac{A_m}{A_p + A_m} \right) = r_i \bar{\theta} \left(1 - \frac{A_p}{aS_0} \right) \quad (15)$$

where

$$\rho_m = r_i \left(\frac{A_m}{A_p + A_m} \right) \quad (16)$$

$$A_p + A_m = aS_0 \quad (17)$$

Here $S_0 = S_i - S_{\text{CMC}}$ and a is a constant (see Table I). According to Omi,⁴

$$A_p = 4.36 \left(\frac{k_2 k_p [\text{A}^0]}{1 - k_1 [\text{A}^0]} \right)^{2/3} \hat{N} N_A \bar{\theta}^{2/3} \quad (18)$$

where

$$k_1 = \frac{v_m M_w}{10^3} \text{ and } k_2 = \frac{v_p M_w}{2N_A} \quad (19)$$

Then

$$\hat{N} = \frac{r_i \bar{\theta}}{1 + \frac{\alpha r_i N_A \bar{\theta}^{5/3}}{aS_0}} \quad (20)$$

where

$$\alpha = 4.36 \left(\frac{k_2 k_p [A^0]}{1 - k_1 [A^0]} \right)^{2/3} \quad S_0 = S_i - S_{\text{CMC}} \quad (21)$$

If the use of eq. (16) is modified by eq. (16'),

$$\rho_m = r_i \left(\frac{\eta A_m}{A_p + A_m} \right) \quad (16')$$

the surface areas of micelles and polymer particles have a different efficiency for capturing the initiator radicals, and η is the correction constant which is experimentally determined by curve fitting the experimental data. The number of polymer particles formed in steady continuous operation is now given by

$$\hat{N} = \frac{\eta r_i \bar{\theta}}{1 + \frac{\eta \alpha r_i N_A \bar{\theta}^{5/3}}{a S_0}} \quad (20')$$

Conversion

Knowledge of the numerical values of k_p and \hat{N} leads to the conversion through eq. (3) as follows:

$$\frac{[M_0]}{\bar{\theta}} - \frac{[M]}{\bar{\theta}} = k_p [A] \hat{P}^* + k_{fM} [A] \hat{P}^* \quad (22)$$

According to Nomura's experimental results, $k_{fM}/k_p = 5.0 \times 10^{-6}$, and thus $k_{fM} = 3.8$ l./mol hr. Thus,²

$$x = \frac{[M_0] - [M]}{[M_0]} = \frac{k_p [A^0] \hat{P}^* \bar{\theta}}{[M_0]} = \frac{0.5 k_p [A^0] \hat{N} \bar{\theta}}{[M_0]} \quad \text{for } x \leq x_{en} = 0.43 \quad (23)$$

Molecular Weight Distribution

Under the steady-state conditions, eq. (4) becomes

$$\begin{aligned} [P_1^*] &= \frac{k_i [K^*] [\hat{N} - \hat{P}^*] + k_{fM} [A] \hat{P}^* + \rho_m}{(1/\bar{\theta}) + k_p [A] + k_i [K^*] + k_{fM} [A]} \\ &= h \beta \end{aligned} \quad (24)$$

where

$$\begin{aligned} h &= \frac{k_i [K^*] [\hat{N} - \hat{P}^*] + k_{fM} [A] \hat{P}^* + \rho_m}{k_p [A]} \\ \beta &= \frac{k_p [A]}{(1/\bar{\theta}) + k_p [A] + k_t [K^*] + k_{fM} [A]} \end{aligned}$$

From eq. (5),

$$\begin{aligned} [P_2^*] &= \frac{k_p [A]}{(1/\bar{\theta}) + k_p [A] + k_t [K^*] + k_{fM} [A]} [P_1^*] \\ [P_2^*] &= h \beta^2 \end{aligned} \quad (25)$$

and

$$[P_3^*] = h\beta^3 \quad (26)$$

$$\vdots$$

$$[P_j^*] = h\beta^j \quad (27)$$

$$\hat{P}^* = \sum_{j=1}^{\infty} [P_j^*] = h \frac{\beta}{1-\beta} \quad (28)$$

The number distribution function is now defined by ν method⁵ as

$$F(j)_n = \frac{[P_j]}{\hat{P}} = \frac{[P_j^*]}{\hat{P}^*} \cong \frac{1}{\nu} \exp\left(-\frac{j}{\nu}\right) \text{ for } \nu \gg 1 \quad (29)$$

The weight distribution function is

$$F(j)_w = \frac{j[P_j]}{\sum j[P_j]} = \frac{j[P_j^*]}{\sum j[P_j^*]} \cong \frac{j}{\nu^2} \exp\left(-\frac{j}{\nu}\right) \text{ for } \nu \gg 1 \quad (30)$$

where

$$\nu = \frac{\beta}{1-\beta} = \frac{k_p[A]}{(1/\bar{\theta}) + k_t[K^*] + k_{fM}[A]}$$

$$= \frac{0.5k_p[A]^0\hat{N}}{k_d\epsilon[I] + 0.5k_{fM}[A]^0\hat{N}} \quad (31)$$

Degree of Polymerization

The number-average degree of polymerization is given by

$$\bar{P}_n = \sum_{j=1}^{\infty} j F(j)_n = \nu \quad (32)$$

The weight-average degree of polymerization is given by

$$\bar{P}_w = \sum_{j=1}^{\infty} j F(j)_w = 2\nu \quad (33)$$

The polydispersity is then given by

$$\bar{M}_w/\bar{M}_n = \bar{P}_w/\bar{P}_n = 2 \quad (34)$$

These performance equations are used to study the kinetics and the design of a continuous emulsion polymerization operation.

EXPERIMENTAL

Materials. Styrene monomer was distilled from industrial-grade styrene under a reduced pressure of about 20 mm Hg. The emulsifier used was sodium lauryl sulfate of extrapure grade. Potassium persulfate of reagent grade was used as the initiator.

Emulsion polymerization. Emulsion polymerization was carried out in a four-neck flask equipped with a two-blade paddle-type impeller, four baffle plates, a thermometer, nitrogen inlet, feed inlet, and condenser. A premixer

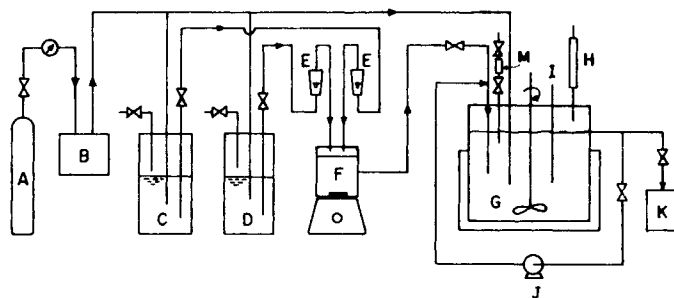


Fig. 1. Flow diagram of polymerization apparatus: A, compressed nitrogen; B, pyrogallol solution, concentrated sulfuric acid, and calcium chloride; C, head tank of styrene; D, head tank of initiator and emulsifier aqueous solution; E, flow meters; F, premixer; G, reactor; H, condenser; I, thermometer; J, recycling pump; K, product sample receiver; M, initiator solution.

was equipped for mixing all components before feed. The polymerization was performed under continuous flow operation with different flow rates and recycle ratios in the apparatus illustrated in Figure 1. The polymerization conditions are listed in Table I.

GPC determination. The MWD and the average degree of polymerization of polymer product were determined by GPC utilizing a Waters Associates instrument model ALC/GPC-200. The pore sizes of five consecutive columns were 500, 10^3 , 10^4 , 10^5 , and 10^6 Å. The flow rate for toluene was 2.0 ml/min, at 23°C. The method proposed by Smith⁶ was used to correct for the GPC instrument spreading.

TABLE I
Polymerization and Numerical Values in Emulsion Polymerization of Styrene^a

Emulsion Polymerization
Sodium lauryl sulfate, 12.50 g/l. water
Potassium persulfate, 1.25 g/l. water
Styrene, 0.50 g/g water
Temperature, 50°C
Numerical Values
$[I_0] = 2.976 \times 10^{-3}$ mol/l.
$k_d \epsilon = 2.394 \times 10^{-3}$ hr ⁻¹
$[M_0] = 3.094$ mol/l.
$k_p = 7.632 \times 10^5$ l./mol hr
$[A^0] = 5.48$ mol/l.
$S_i = 2.79 \times 10^{-2}$ mol/l.
$a = 2.11 \times 10^9$ cm ² /mol
$V_p = 1.0$ cm ³ /g
$V_m = 1.107$ cm ³ /g
$S_{CMC} = 1.116 \times 10^{-3}$ mol/l.
$k_{fM} = 3.8$ l./mol hr
$\eta = 0.4$

^a From Refs. 1, 2, and 3. Most of the constants are adapted from Nomura's data.

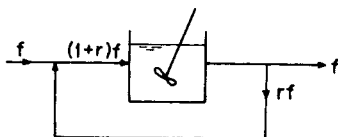


Fig. 2. Notation for a mixing stirred tank with recycle.

RESULTS AND DISCUSSION

A continuous emulsion polymerization by complete mixing in a stirred tank with partial recycling is shown schematically in Figure 2, where r is the recycle ratio and f is the flow rate of reaction mixture.

The relation between the number of polymer particles leaving the reactor and the mean residence time is shown in Figure 3, in which two theoretical curves calculated from eqs. (20) and (20') are cited for comparison. The curve from eq. (20') predicts more closely the experimental number of polymer particles. The difficulty of radical entry into the micelles is due to the higher energy barrier. The initiator radicals have therefore lower efficiency in entering the micelles than the polymer particles.

Figure 4 shows the plot of conversion vs. the mean residence time $\bar{\theta}$ ($= V/f$) for a continuous emulsion polymerization. The solid lines represent the theoretical calculation ($r = 0$ and $r = 1$) by putting the numerical values of Table I into eq. (23). The recycle ratio $r = 0$ represents reaction without recycle. For $r = 1$, half of the stream is returned to the entrance of the reactor. The experimental data (Fig. 4) with the aid of the premixing process are in better agreement with theoretical prediction, while the data without the premixing process yields lower values for both $r = 0$ and $r = 1$. Hence, the apparatus with the premixer performs more complete mixing as assumed in the theoretical treatment. The conversion in the system with recycling always shows higher values than that without recycling or premixing. Thus, recycling provides a means for obtaining more ideal mixing in continuous emulsion polymerization.

The principle of a continuous emulsion polymerization indicates the limitation of the industrial exploitation of the process. Figures 5 and 6 show the rela-

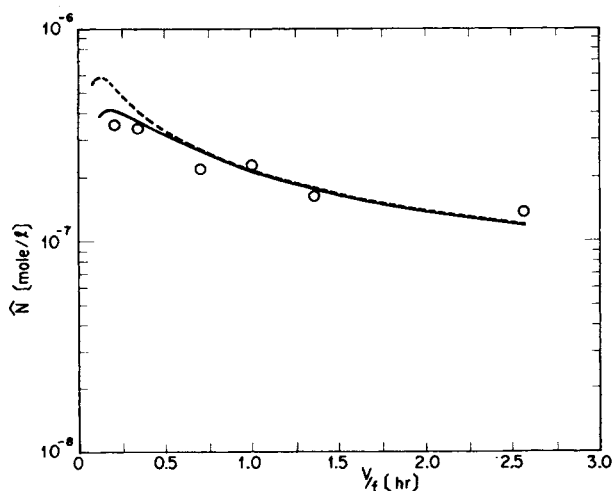


Fig. 3. Relationship between number of polymer particles and mean residence time: (O) Experimental data by Nomura; (---) without correction; (—) with correction.

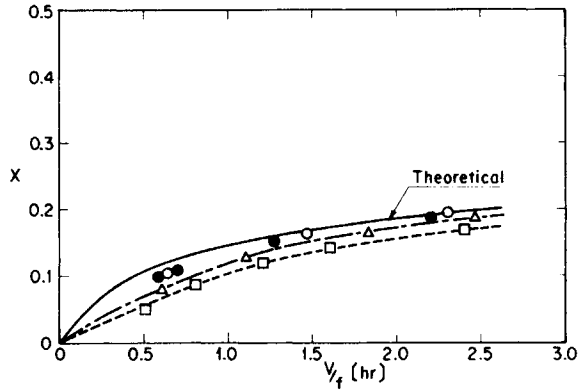


Fig. 4. Relationship between conversion and mean residence time: (Δ) $r = 1.0$ and (\square) $r = 0$, without premixing; (\circ) $r = 1.0$ and (\bullet) $r = 1$, with premixing.

tionships between the degree of polymerization and the mean residence time. The experimental data with premixing are also in better agreement with the theoretical prediction obtained from the performance eqs. (20'), (32), and (33). The experimental data without premixing always give lower molecular weight. Thus, the theoretical curve may be used to estimate the upper boundary for ideal mixing of the process.

Moreover, the calculated chain length is progressively displaced toward a smaller one with a greater mean residence time. Thus, the average molecular weight of polymer obtained decreases as the mean residence time increases. A larger discrepancy between the theoretical and experimental molecular weights is exhibited at shorter residence time. This may be due to the following: (1) the concentration of trace impurities is higher at shorter residence time; (2) the mixing effect at the shorter residence time proves incomplete. Actually, in a

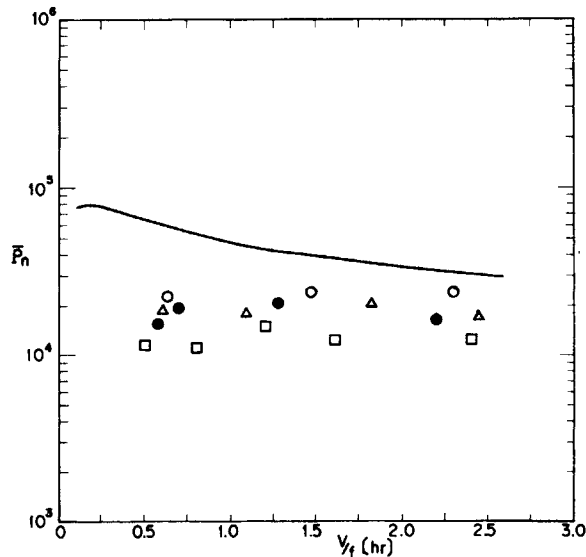


Fig. 5. Number-average degree of polymerization as function of mean residence time: (Δ) $r = 1.0$ and (\square) $r = 0$, with premixing; (\circ) $r = 1.0$ and (\bullet) $r = 0$, with premixing.

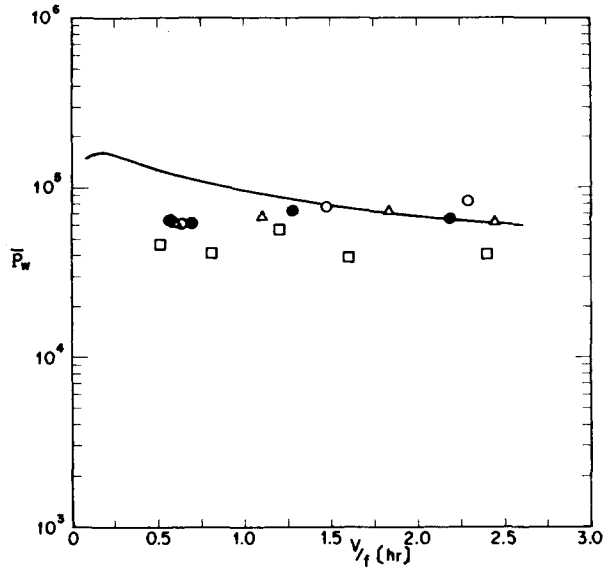


Fig. 6. Weight-average degree of polymerization as function of mean residence time: (Δ) $r = 1.0$ and (\square) $r = 0$, without premixing; (\circ) $r = 1.0$ and (\bullet) $r = 0$, with premixing.

NaCl trace test with our apparatus, the nonideal mixing is observed at the shorter residence time. This fact indicates that the flow proceeds with more "bypass" in the reactor. According to calculations based on the kinetic model, the ratio \bar{M}_w/\bar{M}_n in the continuous emulsion polymerization remains constant. One can obtain a unique polymer product by a continuous emulsion polymerization operation. The \bar{M}_w/\bar{M}_n ratio as a function of the residence time is plotted in Figure 7, where the experimental data show higher values than the theoretical. It results from the nonideal values of \bar{M}_n and \bar{M}_w which are obtained experimentally.

Nomenclature

- α area occupied by a soap molecule (cm^2/mol)
 [A] concentration of monomer dissolved in the polymer particles ($\text{mol/l. polymer particle}$)

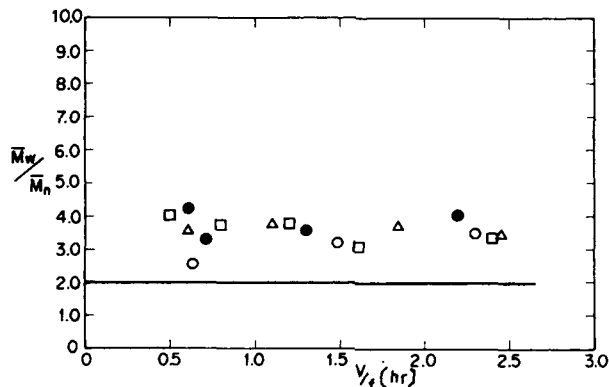


Fig. 7. Relationship between \bar{M}_w/\bar{M}_n and mean residence time: (Δ) $r = 1.0$ and (\square) $r = 0$, without premixing; (\circ) $r = 1.0$ and (\bullet) $r = 0$, with premixing.

$[A^0]$	concentration of monomer above at zero-order stage, a constant (mol/l. polymer particle)
A_m	total surface area of micelles (cm ² /l.)
A_p	total surface area of polymer particles (cm ² /l.)
f	flow rate of reaction mixture (l./hr)
$F(j)_n$	number distribution function (—)
$F(j)_w$	weight distribution function (—)
$[I]$	initiator concentration (mol/l.)
$[I^*]$	concentration of active initiator in the reaction mixture (mol/l.)
$[I_0]$	initiator concentration in feed (mol/l.)
j	number of mers in the polymer chain (—)
k_i	rate constant for initiation based on polymer particle (l./mol hr)
k_d	rate constant for initiator decomposition (hr ⁻¹)
k_{IM}	rate constant of transfer to monomer (l./mol hr)
k_p	rate constant of propagation based on polymer particle (l./mol hr)
k_t	rate constant of termination based on polymer particle (l./mol hr)
$[K^*]$	concentration of active initiator dissolved in polymer particles based on polymer particle (mol/l.)
\bar{M}_n	number-average molecular weight
\bar{M}_w	weight-average molecular weight
$[M]$	monomer concentration (mol/l.)
$[M_0]$	monomer concentration in feed (mol/l.)
M_w	molecular weight of monomer (g/mol)
\bar{N}	total number of polymer particles (mol/l.)
N_A	Avogadro's number
$[P_j^*]$	concentration of polymer radicals (mol/l.)
$[P_j]$	concentration of dead polymer (mol/l.)
\bar{P}_n	number-average degree of polymerization
\bar{P}_w	weight-average degree of polymerization
\bar{P}^*	total concentration of polymer radicals (mol/l.)
\bar{P}	total concentration of dead polymer (mol/l. hr)
r	recycle ratio defined in Figure 2
r_i	effective formation rate of radicals from initiator (mol/l. hr)
S_i	emulsifier concentration in feed or emulsifier concentration initially added (mol/l.)
S_{CMC}	critical micelle concentration (mol/l.)
t	time (hr)
v_m	specific volume of the monomer (cm ³ /g)
v_p	specific volume of the polymer (cm ³ /g)
V	volume of the reactor (liters)
x	monomer conversion
x_{en}	x at time when the reaction shifts from zero-order stage to first-order state
<i>Greek Letters</i>	
$\bar{\theta}$	mean residence time (hr)
ρ_m	rate of diffusion of radicals into micelles (mol/l. hr)
ϵ	efficiency of initiator
η	parameter defined in eq. (16')

References

1. M. Harada, M. Nomura, H. Kojima, W. Eguchi, and S. Nagata, *J. Appl. Polym. Sci.*, **16**, 811 (1972).
2. M. Nomura, H. Kojima, M. Harada, W. Eguchi, and S. Nagata, *J. Appl. Polym. Sci.*, **15**, 675 (1971).
3. C. C. Lin and W. Y. Chiu, *J. Chinese Inst. Chem. Eng.*, **9**, 169 (1978).
4. S. Omi, T. Veda, and H. Kobota, *J. Chem. Eng. Jpn.*, **2**, 193 (1969).
5. Y. Iwasa, S. Rhee, and T. Imoto, *Kagaku Kogaku*, **31**, 373 (1967).
6. W. V. Smith, *J. Appl. Polym. Sci.*, **18**, 925 (1974).

Received March 9, 1979

Revised August 30, 1979